Erschienen in: Current Biology. Cell Press. 2016, 26(6), S. 821-826
https://doi.org/10.1016/j.cub.2016.01.030

Neural Summation in the Hawkmoth Visual System Extends the Limits of Vision in Dim Light

Anna Lisa Stöckl,[1,*] David Charles O'Carroll,[1,2] and Eric James Warrant[1]
[1]Department of Biology, University of Lund, Sölvegatan 35, 22362 Lund, Sweden
[2]Adelaide Centre for Neuroscience Research, The University of Adelaide, Adelaide, SA 5005, Australia
*Correspondence: anna.stockl@biol.lu.se

SUMMARY

Most of the world's animals are active in dim light and depend on good vision for the tasks of daily life. Many have evolved visual adaptations that permit a performance superior to that of manmade imaging devices [1]. In insects, a major model visual system, nocturnal species show impressive visual abilities ranging from flight control [2, 3], to color discrimination [4, 5], to navigation using visual landmarks [6–8] or dim celestial compass cues [9, 10]. In addition to optical adaptations that improve their sensitivity in dim light [11], neural summation of light in space and time—which enhances the coarser and slower features of the scene at the expense of noisier finer and faster features—has been suggested to improve sensitivity in theoretical [12–14], anatomical [15–17], and behavioral [18–20] studies. How these summation strategies function neurally is, however, presently unknown. Here, we quantified spatial and temporal summation in the motion vision pathway of a nocturnal hawkmoth. We show that spatial and temporal summation combine supralinearly to substantially increase contrast sensitivity and visual information rate over four decades of light intensity, enabling hawkmoths to see at light levels 100 times dimmer than without summation. Our results reveal how visual motion is calculated neurally in dim light and how spatial and temporal summation improve sensitivity while simultaneously maximizing spatial and temporal resolution, thus extending models of insect motion vision derived predominantly from diurnal flies. Moreover, the summation strategies we have revealed may benefit manmade vision systems optimized for variable light levels [21].

RESULTS AND DISCUSSION

The impressive visual performance of nocturnal insects is achieved by visual adaptations that minimize the degrading effects of visual noise in dim light. In nocturnal insects, the eyes are typically specialized for high optical sensitivity (e.g., the superposition compound eyes of nocturnal moths; see Figure 2A). Compared to diurnal insects, their photoreceptors have wider spatial receptive fields, slower responses, and approximately five times higher gain, physiological adaptations that improve visual reliability [22, 23]. Potentially, this reliability can be further improved by the neural summation of light in space and time, which enhances the coarser and slower features of the scene at the expense of noisier finer and faster features (Figure 1A). To quantify the costs and benefits of such neural summation strategies, we measured visual performance in the nocturnal hawkmoth *Deilephila elpenor* from the optics and photoreceptors of the eye to wide-field motion-detecting neurons in the optic lobe. We measured the resolution and sensitivity of these motion neurons over a million-fold range of light intensities, from early sunset levels (100 cd/m^2) to starlight (0.0001 cd/m^2). By carefully controlling for the contribution of the superposition pupil and directly comparing spatiotemporal tuning of photoreceptors and motion neurons, we were able to show that spatial and temporal summation are highly beneficial for nocturnal vision, significantly elevating contrast sensitivity over at least four decades of nocturnal light intensity.

Response Characteristics of the Early Visual System

Responses from photoreceptors and direction selective wide-field motion neurons were obtained using moving sinusoidal grating stimuli of different spatial and temporal frequencies (Figure 1B). Photoreceptors responded to this stimulus with sinusoidal modulations in membrane potential, whereas higher-order neurons responded to preferred-direction motion with increased firing rate (Figure 1C; for identities of motion neurons, see Figures S2C–S2H). Grating contrast increased linearly during presentation, allowing quantification of the threshold contrast for a response (50% maximum of a sigmoidal fit to the neural response, C_{50}; see Figure 1D). Unlike neural firing rate at a given contrast, our measure of contrast sensitivity is an estimate of the effective signal-to-noise ratio of the system. Due to the large number of stimulus conditions tested in each neuron, the C_{50} criterion was found to be the most reliable. This measure corresponds to an absolute ''detectability'' criterion [24], with thresholds in our neurons being equivalent to a response increase of between ½ and 1 SD in the firing rate of unstimulated neurons. To determine the contribution of the optics to visual responses, we measured the relative size of the superposition pupil, i.e., the number of ommatidial facet lenses that focus light onto each photoreceptor. In dark-adapted *D. elpenor*, this pupil comprises approximately 500 facets (Table S1), thus increasing retinal illumination by a factor of 500 compared to an apposition compound eye of the same size. Accordingly, the light intensity of the stimulation screen does not necessarily correspond to retinal

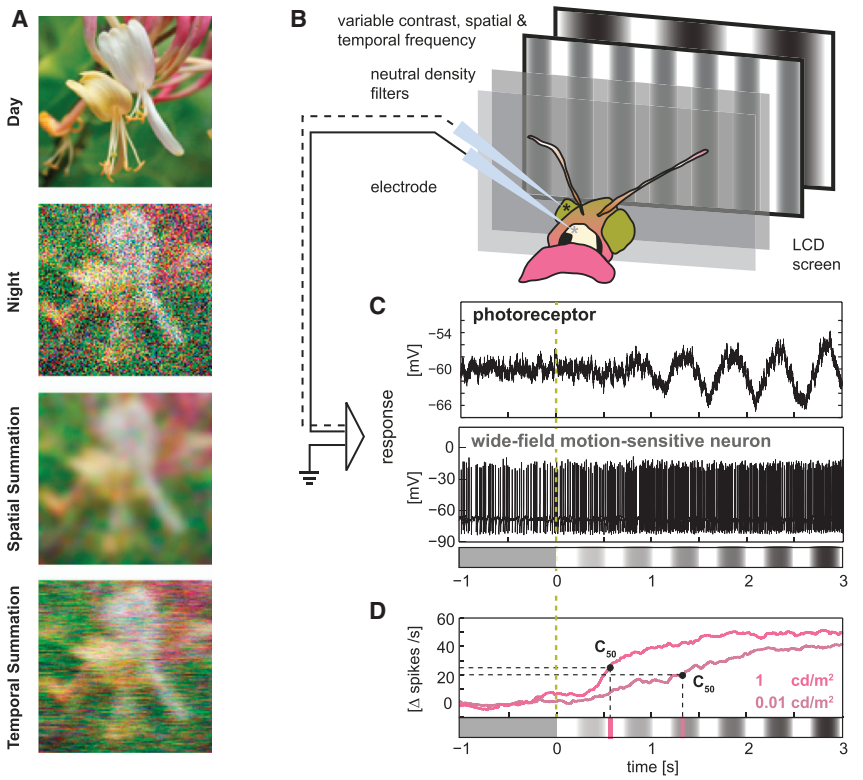

Figure 1. Quantifying Spatial and Temporal Summation

(A) Daytime light intensities allow high-acuity vision, whereas light levels during the night can be so low that noise dominates the visual signal. Summing signals in space or time reduces the noise and boosts the signal, however, at the cost of spatial and temporal resolution. Pixels in the image correspond to visual channels in the moth's eye. Noise levels and spatial and temporal filtering correspond to the measured values at 0.001 cd/m^2.

(B) We recorded from photoreceptors and wide-field motion-sensitive neurons in the hawkmoth *Deilephila elpenor* while stimulating the eyes frontally with moving sinusoidal gratings using an LCD screen. Gratings varied in spatial and temporal frequency and ramped up in contrast in each trial. Light intensity could be controlled with neutral-density filters.

(C) Photoreceptors followed the brightness modulations of the gratings with their membrane potential, whereas motion-sensitive neurons increased their firing rate with increasing contrast of gratings moving in their preferred direction.

(D) Using the half-maximum (C_{50}) of the best sigmoid fit as a threshold, responses of wide-field motion-sensitive neurons were analyzed as contrast sensitivity ($1/C_{50}$).

illumination: at 1 cd/m^2, the pupil was 80% open, paradoxically allowing higher effective retinal illumination than our highest screen intensity (100 cd/m^2) since at this intensity the pupil then closed to a single facet (Figure 2B; Table S2). Below 0.1 cd/m^2, the pupil was fully open (Figure 2B), so retinal illumination became progressively dimmer.

Photoreceptor responses to moving gratings of varying spatial and temporal frequency (Figures 2C and 2E) were similar over a wide range of intensities. The spatial receptive field was slightly broader at the highest intensities but maintained a half-width (acceptance angle, $\Delta\rho$) between 4.2° and 5° over the entire range (Figures 2D, 2F, S1F, and S1G). Temporally, tuning was similar over the brightest four decades of light intensity, evidenced by the almost invariant time course of the temporal impulse response, with a half-width (integration time, Δt) only slightly greater in the fully dark-adapted state (Figures 2D, 2F, S1A, S1C, and S1D).

Response Characteristics of Motion-Sensitive Neurons

At higher light levels, spatiotemporal contrast sensitivity surfaces of motion-sensitive neurons (Figure 3A) had the shape described previously [25–27]. Peak sensitivity occurred at a spatial frequency around 0.05 cycles/degree (Figure 3B) and a temporal frequency below 2 Hz (Figure 3C) with a curious reversal of preferred direction (aliasing) at high temporal frequencies (Figure 3A). At the highest light levels, the upper spatial response limits of motion neurons were clearly set by the spatial limits of photoreceptor responses (dashed white lines, Figure 3A), only falling below these limits at intensities below 0.01 cd/m^2. Temporally, however, response cutoffs were well below photoreceptor limits at all light intensities, indicating substantial neural temporal low-pass filtering between the retina and the lobula plate.

The average peak contrast sensitivity of motion neurons (Figure 3D) remained above 15 (indicating discrimination of contrasts below 7%) over four decades of screen intensity, from sunset to full-moonlight levels. This remarkably consistent performance reveals the action of nocturnal visual adaptations: without them, contrast sensitivity should fall with the square root of light intensity [28, 29] and thus decrease 100-fold over four decades (see Figure 3D).

Both peak spatial frequency and contrast sensitivity (Figures 3B and 3D) were lower at the two highest light intensities (when the pupil was fully or partly closed; Figure 2B) than at 1 cd/m^2, with a fully open pupil. The spatial peak then decreased with decreasing intensity (Figure 3B). In contrast, the temporal peak remained stable over the brightest four decades, slightly decreasing as light levels fall further, whereas the cutoff (corner) frequency gradually decreased over the entire intensity range, indicating continuous changes in temporal tuning (Figure 3C).

How Much Spatial and Temporal Summation Does the Visual System Use?

The intensity-dependent changes in spatial and temporal tuning that we measured in motion-sensitive neurons indicate coarser tuning than concomitant changes in photoreceptor tuning (particularly in the time domain), implying additional spatial and temporal summation of visual signals between the retina and lobula plate. To quantify the extent of this intermediate summation, we fitted a computational motion model to the tuning

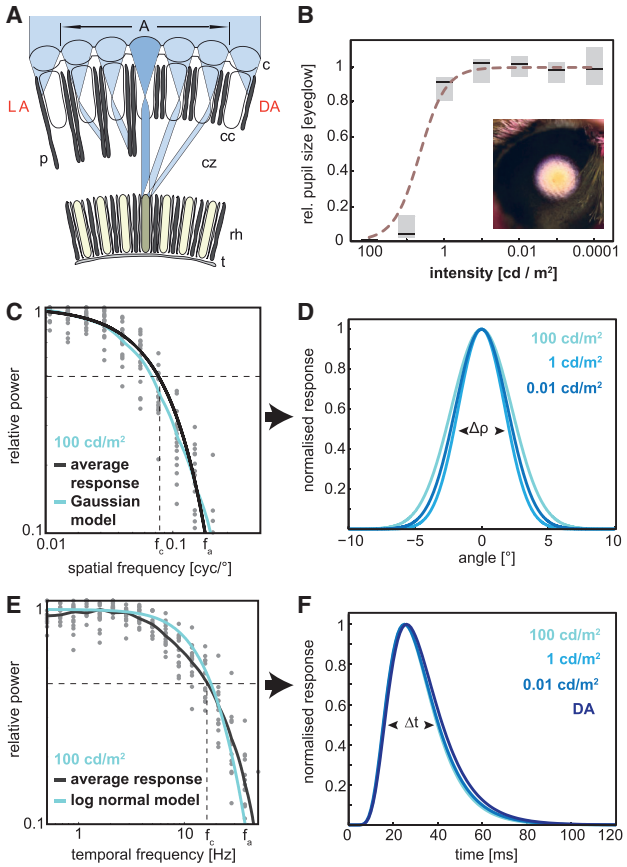

Figure 2. Photoreceptor Spatial and Temporal Characteristics

(A) The hawkmoth's superposition compound eye. In the extreme light-adapted state (LA), a single corneal lens (c) and crystalline cone (cc) focus light from facets through the clear zone (cz) onto the photoreceptors (rh) of one ommatidium in the retina, because pigment (p) extending into the cz prevents light from reaching neighboring ommatidia. In the dark-adapted state (DA), the pigment retracts and the cc of multiple facets collect light from one point in space onto one rhabdom, thus increasing the effective aperture (A). t, tapetum.

(B) Eyeglow, the light reflected from a tapetum (formed by trachea surrounding the rhabdoms; see inset), was used to measure the relative size of the pupil. Shown is the median data with interquartile range (gray shading) and best sigmoid fit (dashed line).

(C and E) Responses of photoreceptors to spatial (C) and temporal (E) frequency gratings, measured as relative power of the grating's temporal frequency, at 100 cd/m^2. Individual photoreceptor responses (gray dots), averages (black curves), best-fit Gaussian model of receptive field (C, blue curve), best-fit lognormal model of the impulse response (E, blue curve), and corner frequency f_c (dashed lines) are shown.

(D and F) Best-fit Gaussian models of photoreceptor spatial receptive fields (D) and lognormal models of photoreceptor impulse responses (F) at 100, 1, and 0.01 cd/m^2 extracted from their responses to sinusoidal gratings.

See also Figures S1, S2A, and S2B.

of motion responses at different light intensities (Figure 4A). A sinusoidal stimulus was first filtered with the measured spatial and temporal properties of the photoreceptors (Figures 2E and 2F). Hypothetical spatial and temporal summation was then modeled as additional spatial and temporal low-pass filters, whose parameters were fitted to the physiological responses of motion neurons (see [30]). The spatial low-pass filter was a Gaussian function with a variable half-width, whereas the temporal filter was a variable exponential (first-order) low-pass filter. Signals were subsequently passed through a correlator-type elementary motion detector (EMD) with a fixed exponential delay (see the Supplemental Experimental Procedures and Figures S3C–S3E).

At 100 cd/m^2, the half-width of the spatial summation filter remained well below that of the photoreceptor spatial kernel (Figure 4B). This indicates that although there was a constant low level of spatial summation, the spatial properties of the motion neurons were mainly shaped by peripheral, rather than central, mechanisms at brighter light levels. Since the photoreceptor acceptance angle (~4.5°) is around four times the interommatidial angle (1.12° [17]), the visual scene is spatially oversampled. As a result, low levels of spatial summation at these light intensities did not reduce spatial acuity, but rather increased sensitivity while simultaneously reducing the spatial oversampling. At light intensities below 0.01 cd/m^2, substantial spatial summation was necessary to explain the tuning of the motion neurons. By 0.0001 cd/m^2, the average spatial summation was estimated as a Gaussian with a half-width of 11° of visual angle, implying summation of signals from 109 neighboring ommatidia. Thus, our results suggest that hawkmoths optimize spatial resolution by performing only moderate spatial summation at higher light intensities, whereas at lower light intensities—when maximizing sensitivity becomes a priority—spatial summation is increased, thereby reducing spatial resolution.

In the temporal domain, a different picture arose: the time constant of the summation filter remained constant at 100 ms for the brightest four decades of light intensity. This is over four times longer than the time constant of the photoreceptors over the same range, indicating substantial temporal summation in the optic lobe at higher light intensities (Figure 4C). For intensities below 0.01 cd/m^2, the time constant lengthened even further to 220 ms (see also Figure 3A). Thus, these hawkmoths perform substantial amounts of temporal summation at all light intensities, decreasing their temporal resolution well below the limits of their photoreceptors. Thus, their permanently low temporal optima might serve purposes in addition to increasing visual sensitivity. As suggested by O'Carroll and colleagues [26, 27], slow temporal tuning in the motion vision pathway of hawkmoths might be an adaptation for hovering flight, and thus the need for both high sensitivity and accurate hovering may have selected for low temporal tuning.

Our results are in good agreement with recent behavioral experiments in the hawkmoth *Manduca sexta* showing that good flight performance at falling light levels can only be maintained by an increasingly slower motion system [20]. Moreover, the minimum intensity at which our motion sensitive neurons responded (10^{-4} cd/m^2) is also the lowest intensity at which *D. elpenor* is able to distinguish color using its trichromatic visual system (as measured in behavioral experiments [4]). Since the moths were flying during these behavioral experiments (and were thus using their motion-sensitive flight control system), their behavioral and physiological light-intensity limits are in good agreement. Furthermore, since we found substantial amounts of spatial and temporal summation in the motion pathway at light intensities below 10^{-4} cd/m^2, it seems logical to conclude that similar

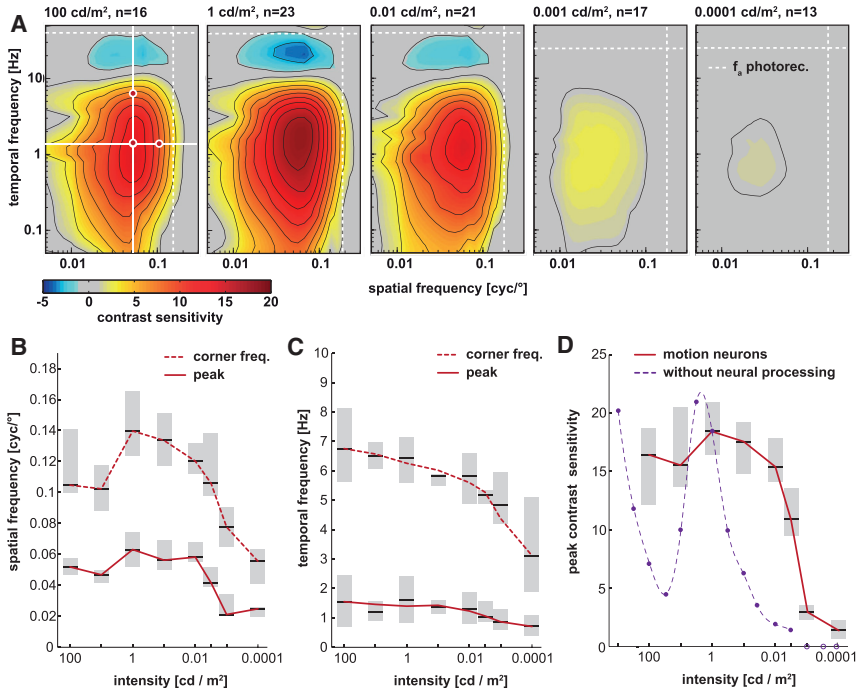

Figure 3. Spatial and Temporal Characteristics of Motion-Sensitive Neurons

(A) Contrast sensitivity response surfaces of wide-field motion-sensitive neurons. Peak and 50% cutoff (corner) frequency at the best spatial and temporal frequency (solid lines, first panel) and absolute cut-off frequencies of photoreceptors (f_a, dashed lines) are shown.

(B and C) Spatial (B) and temporal (C) peak and corner frequencies of wide-field motion-sensitive neurons at different light intensities.

(D) Peak contrast sensitivity at different light intensities in wide-field motion-sensitive neurons (red curve) and modeled motion-sensitive neurons without summation (purple curve; condition "NO" in Figure 4D; data are normalized and scaled to the physiological data at 1 cd/m^2).

(B–D) Median (black line) and interquartile range (gray shaded) are shown.

See also Figure S2.

neural summation strategies might also be employed in the color pathway, thus permitting color vision at these low light levels.

The Effect of Neural Summation on Visual Reliability

We are now in a position to ask whether the significant spatial and temporal summation predicted by our motion model can explain the high contrast sensitivity maintained by motion neurons as light levels fall (Figure 3D). In order to add realistic levels of noise to the model input signals, we calculated photon shot noise at each experimental light intensity (see Tables S1 and S2 for green-sensitive photoreceptors; Figures S2A and S2B). Because the effects of thermal noise (likely to be negligible [31]) and transducer noise in hawkmoth photoreceptors are unknown, we decided to focus on photon shot noise, thus modeling the best-case scenario for the visual system. Nonetheless, we can estimate the added effects of transducer noise by recognizing that the total noise at any given light level (photon shot noise + transducer noise) will have the same magnitude as photon shot noise alone at a dimmer light level. For instance, if the magnitudes of the transducer noise and the photon shot noise are equal (as in locusts at low light intensities [32]), the model results would be the same as those obtained for photon shot noise alone at a light intensity that is four times dimmer.

We modeled input signals that ramp in contrast (as in our experiments) and then calculated contrast sensitivity using a noise-based threshold on model outputs. This allowed us to obtain both contrast sensitivity and the information rate of the response (Figures 4D and 4E). We ran different model variants with or without summation filters: "NO" (a simple EMD control with no additional summation), "SS" (spatial summation), "TS" (temporal summation), and "STS" (spatial and temporal summation, using estimated parameters at 0.001 cd/m^2). We also tested a variant, "INT," with spatial integration of 30 individual EMDs, as occurs at the dendrites of wide-field motion-sensitive neurons in the lobula plate [33] and one ("ALL") with all three types of pre- and post-EMD summation.

At both high and low light intensities (100 cd/m^2 and 0.001 cd/m^2), all summation models increased contrast sensitivity compared to the control, particularly at lower light intensities (Figures 4D and S4). Integration over multiple EMDs (INT) increased contrast sensitivity only marginally at either intensity (see also Table S3), illustrating the importance of reducing noise at early stages in visual processing, prior to the nonlinear EMDs (see [34]). Temporal summation alone (TS) did not significantly increase sensitivity, whereas spatial summation (SS) did, having the advantage of integrating the signal from several neighboring channels with uncorrelated noise. However, when combined (ALL), spatial summation, temporal summation, and EMD integration increased contrast sensitivity supralinearly (i.e., by a factor larger than expected from the linear sum of their isolated contributions), especially at low light intensities, indicating the benefit of having all these mechanisms in place.

The model so far only accounts for photoreceptor noise; however, noise could arise at several stages in the neural pathway. The contributions of such downstream neuronal noise to the motion vision system have been discussed previously: the housefly (*Musca domestica*), tethered within a rotating optomotor drum lined with vertical stripes, reacts to the movements of these stripes when as few as two or three photons reach each photoreceptor every second [35], suggesting that photoreceptor noise is the limiting factor on performance. However, it was demonstrated that at higher light intensities, the main response variance in motion-sensitive neurons of blowflies does not result from photon shot noise, but from other sources of neuronal noise [36]. In order to test the effect of downstream neuronal noise on our model, we added moderate levels of Gaussian noise (at 5% of the input signal) after the spatial and temporal filters but

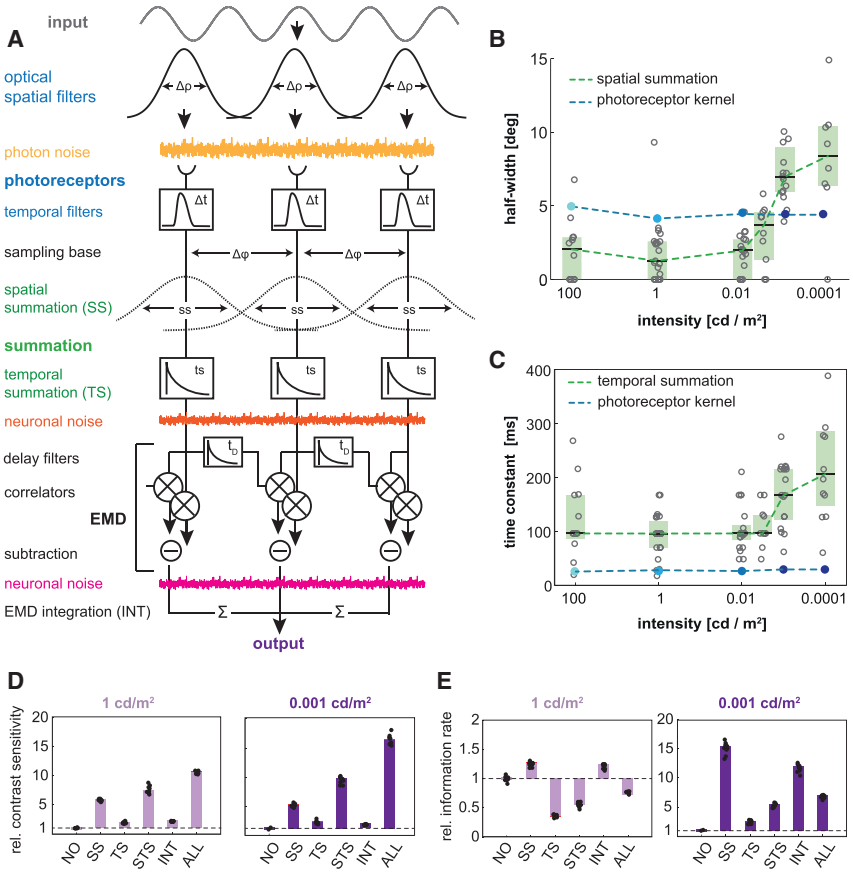

Figure 4. The Effects of Neural Summation in the Hawkmoth Visual System

(A) Model of hawkmoth motion vision. A sinusoidal signal is spatially filtered by the eye's optics ($\Delta\rho$). Photon noise (yellow) is added, which is temporally filtered by the photoreceptors (Δt) at a spatial sampling base of one interommatidial angle ($\Delta\varphi$). Spatial summation is implemented as a Gaussian filter (SS) and temporal summation as an exponential filter (TS). The signal then passes through an elementary motion detector (EMD) with a first-order delay filter (t_D), and, finally, multiple EMD outputs are integrated. Downstream neuronal noise can be added before (orange) and after (pink) the EMDs, respectively.

(B) Model estimates of the angular half-width of spatial low-pass filters (green) and the photoreceptor acceptance angle $\Delta\rho$ (blue) at different light intensities.

(C) Model estimates of the time constants of temporal low-pass filters (green) and photoreceptor time constants (blue) at different light intensities.

(B and C) Median (black line) and interquartile range (shaded) are shown.

(D and E) The modeled effect on contrast sensitivity (D) and information rate (E) at 1 and 0.001 cd/m^2 of spatial summation (SS), temporal summation (TS), the two combined (STS), integration of 30 EMDs (INT), and a combination of all these (ALL) compared to the pure output of the EMD model (NO). Noise is added to reflect the system's photon shot noise. Values are normalized to the NO condition.

See also Figures S3 and S4 and Tables S1–S3.

before the EMD correlation step (Figure 4A, red) and in a second test after the EMD step (Figure 4A, pink). In both cases, sensitivity at the lowest light intensities was only maintained with neural summation, demonstrating that even with moderate levels of added neuronal noise, photon shot noise remains the limiting factor for vision at low light intensities and that neural summation is crucial to restore sensitivity. However, the contribution of neural summation to sensitivity at higher light intensities was reduced with the addition of neuronal noise (Figures S4C and S4D). Moreover, spatial integration (INT) played a bigger role in reducing noise and increasing contrast sensitivity when neuronal noise is present, compared to photoreceptor noise only (Figures S4C and S4D).

Even though summation only increases sensitivity at the cost of resolution [3, 14], our model shows that the amount of information the visual system can code at different light levels (which depends on resolution *and* sensitivity) nonetheless significantly increases with summation at low light intensities (Figures 4E and S4). In fact, over four decades of nocturnal light intensity, modeled contrast sensitivity (based on the best-case noise estimate) is dramatically worse if summation is absent, falling to zero at light levels 100 times brighter (Figure 3D).

Conclusions

In conclusion, we have physiologically quantified spatial and temporal summation in a nocturnal insect and showed that both are highly beneficial for vision in dim light. Summation maintains high contrast sensitivity over a broad range of nocturnal light intensities, thereby restoring the visibility of coarser and slower details in the visual scene that would otherwise be drowned by noise. We expect these neural adaptations to be widespread in nocturnal animals, particularly those similar to insects, with small eyes and brains. Moreover, these strategies may be of benefit not only to animals, but also to manmade seeing systems optimized for variable light levels, by implementing algorithms that mimic these strategies in video processing software [1].

AUTHOR CONTRIBUTIONS

Conceptualization, E.J.W. and D.C.O.; Methodology, A.L.S., D.C.O., and E.J.W.; Investigation, A.L.S.; Formal Analysis, A.L.S. and D.C.O.; Writing – Original Draft, A.L.S.; Writing – Review & Editing, A.L.S., D.C.O., and E.J.W.; Visualization: A.L.S.; Funding Acquisition, E.J.W. and D.C.O.; Resources, E.J.W. and D.C.O.; Supervision, E.J.W. and D.C.O.

ACKNOWLEDGMENTS

This research was supported by the Swedish Research Council (VR 621-2012-2205), The Knut and Alice Wallenberg Foundation, the Australian

Research Council's Discovery Projects funding scheme (project number DP130104561), and the Swedish Foundation for International Cooperation in Research and Higher Education (STINT 2012-2033). We would like to thank David Liittschwager for providing the moth image used in the graphical abstract.

REFERENCES

1. Warrant, E., Oskarsson, M., and Malm, H. (2014). The remarkable visual abilities of nocturnal insects: neural principles and bioinspired night-vision algorithms. Proc. IEEE *102*, 1411–1426.
2. Baird, E., Kreiss, E., Wcislo, W., Warrant, E., and Dacke, M. (2011). Nocturnal insects use optic flow for flight control. Biol. Lett. *7*, 499–501.
3. Theobald, J.C., Coates, M.M., Wcislo, W.T., and Warrant, E.J. (2007). Flight performance in night-flying sweat bees suffers at low light levels. J. Exp. Biol. *210*, 4034–4042.
4. Kelber, A., Balkenius, A., and Warrant, E.J. (2002). Scotopic colour vision in nocturnal hawkmoths. Nature *419*, 922–925.
5. Somanathan, H., Borges, R.M., Warrant, E.J., and Kelber, A. (2008). Nocturnal bees learn landmark colours in starlight. Curr. Biol. *18*, R996–R997.
6. Reid, S.F., Narendra, A., Hemmi, J.M., and Zeil, J. (2011). Polarised skylight and the landmark panorama provide night-active bull ants with compass information during route following. J. Exp. Biol. *214*, 363–370.
7. Somanathan, H., Borges, R.M., Warrant, E.J., and Kelber, A. (2008). Visual ecology of Indian carpenter bees I: light intensities and flight activity. J. Comp. Physiol. A Neuroethol. Sens. Neural Behav. Physiol. *194*, 97–107.
8. Warrant, E.J., Kelber, A., Gislén, A., Greiner, B., Ribi, W., and Wcislo, W.T. (2004). Nocturnal vision and landmark orientation in a tropical halictid bee. Curr. Biol. *14*, 1309–1318.
9. Dacke, M., Nilsson, D.E., Scholtz, C.H., Byrne, M., and Warrant, E.J. (2003). Animal behaviour: insect orientation to polarized moonlight. Nature *424*, 33.
10. Dacke, M., Baird, E., Byrne, M., Scholtz, C.H., and Warrant, E.J. (2013). Dung beetles use the Milky Way for orientation. Curr. Biol. *23*, 298–300.
11. Warrant, E., and Dacke, M. (2011). Vision and visual navigation in nocturnal insects. Annu. Rev. Entomol. *56*, 239–254.
12. Klaus, A., and Warrant, E.J. (2009). Optimum spatiotemporal receptive fields for vision in dim light. J. Vis. *9*, 1–16.
13. Theobald, J.C., Greiner, B., Wcislo, W.T., and Warrant, E.J. (2006). Visual summation in night-flying sweat bees: a theoretical study. Vision Res. *46*, 2298–2309.
14. Warrant, E.J. (1999). Seeing better at night: life style, eye design and the optimum strategy of spatial and temporal summation. Vision Res. *39*, 1611–1630.
15. Greiner, B., Ribi, W.A., and Warrant, E.J. (2004). Retinal and optical adaptations for nocturnal vision in the halictid bee Megalopta genalis. Cell Tissue Res. *316*, 377–390.
16. Greiner, B., Ribi, W.A., and Warrant, E.J. (2005). A neural network to improve dim-light vision? Dendritic fields of first-order interneurons in the nocturnal bee Megalopta genalis. Cell Tissue Res. *322*, 313–320.
17. Stöckl, A.L., Ribi, W.A., and Warrant, E.J. (2016). Adaptations for nocturnal and diurnal vision in the hawkmoth lamina. J. Comp. Neurol. *524*, 160–175.
18. Honkanen, A., Takalo, J., Heimonen, K., Vähäsöyrinki, M., and Weckström, M. (2014). Cockroach optomotor responses below single photon level. J. Exp. Biol. *217*, 4262–4268.
19. Reber, T., Vähäkainu, A., Baird, E., Weckström, M., Warrant, E., and Dacke, M. (2015). Effect of light intensity on flight control and temporal properties of photoreceptors in bumblebees. J. Exp. Biol. *218*, 1339–1346.
20. Sponberg, S., Dyhr, J.P., Hall, R.W., and Daniel, T.L. (2015). Luminance-dependent visual processing enables moth flight in low light. Science *348*, 1245–1248.
21. Wiederman, S., and O'Carroll, D. (2013). Biomimetic target detection: modeling 2nd order correlation of OFF and ON channels. In Computational Intelligence for Multimedia 2013, IEEE Symposium on Signal and Vision Processing (CIMSIVP), pp. 16–21.
22. Laughlin, S., and Weckström, M. (1993). Fast and slow photoreceptors: a comparative study of the functional diversity of coding and conductances in the Diptera. J. Comp. Physiol. A *172*, 593–609.
23. Frederiksen, R., Wcislo, W.T., and Warrant, E.J. (2008). Visual reliability and information rate in the retina of a nocturnal bee. Curr. Biol. *18*, 349–353.
24. Dvorak, D., Srinivasan, M.V., and French, A.S. (1980). The contrast sensitivity of fly movement-detecting neurons. Vision Res. *20*, 397–407.
25. Theobald, J.C., Warrant, E.J., and O'Carroll, D.C. (2010). Wide-field motion tuning in nocturnal hawkmoths. Proc. Biol. Sci. *277*, 853–860.
26. O'Carroll, D.C., Bidwell, N.J., Laughlin, S.B., and Warrant, E.J. (1996). Insect motion detectors matched to visual ecology. Nature *382*, 63–66.
27. O'Carroll, D.C., Laughlin, S.B., Bidwell, N.J., and Harris, R.A. (1997). Spatio-temporal properties of motion detectors matched to low image velocities in hovering insects. Vision Res. *37*, 3427–3439.
28. De Vries, H. (1943). The quantum character of light and its bearing upon threshold of vision. Physica *10*, 553–564.
29. Rose, A. (1942). The relative sensitivities of television pickup tubes, photographic film, and the human eye. Proc. IRE *30*, 293–300.
30. O'Carroll, D.C., and Warrant, E.J. (2011). Computational models for spatiotemporal filtering strategies in insect motion vision at low light levels. In 2011 Seventh International Conference on Intelligent Sensors, Sensor Networks and Information Processing (ISSNIP), pp. 119–124.
31. Katz, B., and Minke, B. (2012). Phospholipase C-mediated suppression of dark noise enables single-photon detection in Drosophila photoreceptors. J. Neurosci. *32*, 2722–2733.
32. Laughlin, S.B., and Lillywhite, P.G. (1982). Intrinsic noise in locust photoreceptors. J. Physiol. *332*, 25–45.
33. Single, S., and Borst, A. (1998). Dendritic integration and its role in computing image velocity. Science *281*, 1848–1850.
34. van Hateren, J.H. (1992). A theory of maximizing sensory information. Biol. Cybern. *68*, 23–29.
35. Dubs, A. (1981). Non-linearity and light adaptation in the fly photoreceptor. J. Comp. Physiol. *144*, 53–59.
36. Grewe, J., Kretzberg, J., Warzecha, A.K., and Egelhaaf, M. (2003). Impact of photon noise on the reliability of a motion-sensitive neuron in the fly's visual system. J. Neurosci. *23*, 10776–10783.